Multi-Bit & Sequential Decentralized Detection of a Noncooperative Moving Target Through a Generalized Rao Test

Xu Cheng , *Member, IEEE*, Domenico Ciuonzo , *Senior Member, IEEE*,
Pierluigi Salvo Rossi , *Senior Member, IEEE*, Xiaodong Wang , *Fellow, IEEE*, and Wei Wang

Abstract—We consider decentralized detection (DD) of an uncooperative moving target via wireless sensor networks (WSNs), measured in zero-mean unimodal noise. To address energy and bandwidth limitations, the sensors use multi-level quantizers. The encoded bits are then reported to a fusion center (FC) via binary symmetric channels. Herein, we propose a generalized Rao (G-Rao) test as a simpler alternative to the generalized likelihood ratio test (GLRT). Then, at the FC, a truncated one-sided sequential (TOS) test rule is considered in addition to the fixed-sample-size (FSS) manner. Further, the asymptotic performance of a trajectory-clairvoyant (multi-bit) Rao test is leveraged to develop an offline and per-sensor quantizer design. Detection gain measures are also introduced to assess resolution improvements. Simulations show the appeal of G-Rao test with respect to the GLRT, and the gain in detection by using multiple bits for quantization, as well as the advantage of the sequential detection approach.

Index Terms—Decentralized detection, generalized Rao test, multibit quantizer, sequential detection, wireless sensor networks.

I. INTRODUCTION

A. Motivation and Related Works

THE study on Decentralized Detection (DD) started from 1980s [1], [2] and has received significant attention in Wireless Sensor Networks (WSNs) area by the scientific community over the last two decades [3]–[11]. Nowadays, DD is the object of renewed interest with the advent of the Internet of Things (IoT) paradigm. Indeed, billions of tiny devices with sensing, computation, and communicating capabilities are expected to be used in numerous areas of everyday life, such as surveillance, environmental monitoring, smart cities and grids, connected cars, precision-agriculture and healthcare.

A WSN with a centralized architecture typically consists of a large number of spatially-distributed sensors and a Fusion Center (FC). The sensors collect measurements of a given physical process (temperature, humidity, etc.) or, in case of DD, are in charge of detecting (together) some specific events in a region of interest [12]. These may correspond to target/signal presence or anomalies, e.g. deviations from normal behavior attributed to unforeseen changes in the system/environment. Last but not least, sensor nodes are usually subject to energy and/or bandwidth limitations. Therefore, they may be compelled to *quantize* their measurements (into one or more bits), before reporting them to the FC [13].

In DD case, the optimal per-sensor digital compression (under Bayesian/Neyman-Pearson frameworks) corresponds to a quantization of the local Likelihood-Ratio (LR) [14], [15]. Unfortunately, incomplete knowledge of the parameters of the event to be detected precludes the sensors from computing local LRs. Additionally, the search for quantization thresholds is exponentially complex [16]. Thus the bit sent is either the result of a "dumb" quantization [17] or embodies the estimated binary event, based on a sub-optimal rule [18].

In both cases sensors' bits are sent to the FC, where they are fused via an intelligently-designed rule meant to overcome sensors' limited detection capabilities. Therein a system-wide decision (based on a so-called *fusion rule*) is taken [18], [19], which is object of design efforts. Sadly, the target (or event) to be detected depends on some unknown parameters. This precludes (global) LR implementation at FC [16], which is then faced to test a composite hypothesis.

A commonly-adopted fusion rule in such cases corresponds to the Generalized LR Test (GLRT) [20]–[22]. Due to its wide applicability, GLRT-based fusion rules have been also devised in a number of different scenarios, such as arbitrarily-permuted quantized data [23] and sparse signals [24]. On the other hand, one appealing alternative (suited to two-sided tests[1]) is represented by the adoption of *Rao-based fusion rules* [17], [26], [27], which usually incurs lower computational costs. For instance, in [17], a one-bit Rao fusion rule is proposed as a simpler (from

[1]Instead, for one-sided tests, (generalized) locally most-powerful detectors are usually preferred [11], [25].

a computational viewpoint) alternative to the one-bit GLRT for detection of an unknown signal. More recently, a Rao test is applied to fusion rule design in the case of collision-aware reporting channels [26] and vector-valued measurements [27], respectively. We remark that an alternative (appealing) path for designing effective distributed detectors is also represented by the exploitation of invariance properties, see e.g., [28], [29].

Referring to an unknown two-sided signal and both rationales, quantizer threshold(s) design can be performed via their *common* (weak-signal) asymptotic performance [30]. In the one-bit case, it has been shown that the optimal threshold value corresponds to zero in many practical cases, except for some heavy-tailed distributions, such as the Generalized Gaussian Distribution (GGD) [17], [20], [31]. In the latter case, the study in [32] provided a threshold optimization algorithm for GGD noise with polynomial-time guarantees.

Yet, in the case of an unknown static (resp. moving) target with unknown location (resp. trajectory), the GLRT requires a grid search on both the target location (trajectory) and emitted signal domains. Hence, the search for simpler fusion rules is even *exacerbated*. Accordingly, recent works have devised a *generalized* Rao test for one-bit DD of uncooperative targets in finite-sample [33] and sequential [34] setups. The aforementioned generalized forms overcome the technical issue of unidentifiable nuisance parameters under $\mathcal{H}_0$, and corresponding to the location (resp. trajectory) of the target to be detected. Also, the corresponding quantizer design can be obtained via the optimization of location- (resp. trajectory-) clairvoyant performance which, remarkably, *does not depend on the aforementioned (unknown) parameters* [33], [34].

There is however a tangible *loss of useful information when only one-bit quantizers are adopted* and a notable performance gap can be observed with respect to unquantized observations [35]. Accordingly, *multi-level quantization* can be adopted to achieve performance gains at the expenses of a mild complexity increase. Based on this idea, multi-bit DD has been recently considered for the simpler scenario of an unknown (two-sided) signal in Gaussian [36] and zero-mean unimodal symmetric noise [37], respectively. Therein *multi-bit GLR (not in closed-form)* and Rao tests (*in closed-form*), respectively, have been devised and an asymptotically-optimal thresholds' design obtained, via a Particle Swarm Optimization (PSO) [38]. Numerical results therein have demonstrated that 2/3-bit quantization suffices for both fusion rules to approach the performance of their unquantized counterparts. Accordingly, it is of interest investigating (*a*) multi-bit quantizers, (*b*) their corresponding design and (*c*) the derivation of computationally-efficient fusion rules for the challenging case of a non-coooperative (moving) target. This is the objective of the present work.

B. Contributions and Paper Organization

The main contributions of this paper are summarized as follows:
- We study the problem of DD of a *non-cooperative* moving target buried in noise via WSNs [11], [33], [39]. To cope with WSNs stringent energy & bandwidth budgets, we

consider *multi-level quantized* sensors. Also, we assume the quantized data to be transmitted through (error-prone) Binary Symmetric Channels (BSC) to the FC, similarly as in [36], [37]. However, as opposed to [36], [37], we tackle the (challenging) task of detecting a target with unknown location. Additionally, similarly to [37], we *only constrain the noise to be zero-mean unimodal-symmetric*. The resulting test is two-sided with nuisance parameters present only under hypothesis $\mathcal{H}_1$, thus making inapplicable the standard Rao test [37].

- To circumvent this issue, we devise *a multi-bit form of the generalized Rao test* (G-Rao), representing (*i*) a (computationally-) simpler alternative *fusion rule* to the GLRT and (*ii*) comprising the one-bit G-Rao devised in [33] as a special case, although it does not represent a trivial extension of the above simplified scenario. Indeed, the main advantage is that it *requires* a reduced estimation procedure [30] even in the considered general model. At the FC, we consider both *Fixed-Sample-Size* (FSS) and *sequential* test rules, to exhibit their properties and highlight the advantage of the latter (thus generalizing the findings of [34] for the one-bit case).

- We provide the asymptotic (weak-signal) performance of the *trajectory-clairvoyant* (TC) Rao test. Leveraging its explicit expression, we adopt a quantizer design approach for the sensors which aims at maximizing the corresponding *non-centrality parameter*. Such design is per-sensor, accounts for sensor-FC channel status, and requires neither the target signal nor its trajectory. Hence, the proposed design is *feasible* and can be computed *offline* via PSO (following [36], [37]). Then, in the FSS setup, the TC asymptotic performance is capitalized to define asymptotic detection gains (ADGs), which concisely allow to quantify the gain on WSN system performance achieved by increasing the bit resolution of sensors within the network.

- Finally, the G-Rao test is compared to the GLRT through simulations (pertaining to relevant Gaussian and Generalized Gaussian noise cases) showing that it achieves practically the same performance for a finite number of sensors in the considered scenarios[2].

We highlight that the present work extends our earlier conference paper [40], which provided (*i*) only a *preliminary analysis* of PSO-based quantizer optimization, (*ii*) considered *only the FSS setup* and (*iii*) did not introduce ADGs of TC Rao test (as well as TC GLRT) versus resolution. Besides, we also clarify that our previous work [37] focuses on the DD of *an unknown signal* with known observation coefficients (able to accommodate only targets with known position/trajectory) with *a multi-bit Rao test*.

The rest of the manuscript is organized as follows. Section II introduces the model; in Section III the multi-bit G-Rao (resp. GLR) test is derived (resp. recalled), and the fusion rule is formulated under both FSS and sequential setups; in Section IV,

---

[2]Actually, in most of the cases, the G-Rao test slightly outperforms the GLRT (see Section VI). This is not counterintuitive, as the finite-sample relative performance of GLR and Rao tests varies from case to case, even in the simpler two-sided testing (i.e. without nuisance parameters under $\mathcal{H}_1$). Indeed, in the latter case, their performance is only asymptotically equivalent, see [30].
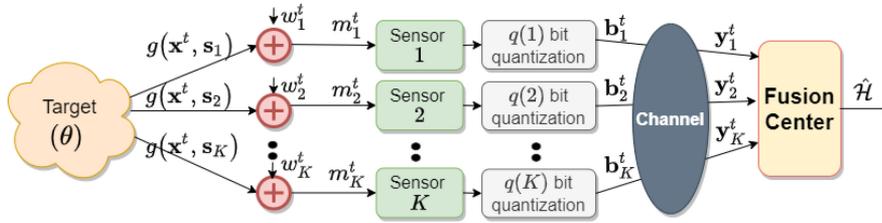
Fig. 1.   WSN system model with multi-bit and error-prone sensors detecting a non-cooperative moving target.

an asymptotic analysis of the multi-bit TC Rao (GLR) detector is presented, and PSO-based multi-level quantizers are developed; performance analysis versus resolution of quantization is investigated in Section V, while numerical results are provided in Section VI. Finally, concluding remarks and further avenues of research are given in Section VII. Additional proofs are deferred to dedicated appendices.

Notation - vectors are denoted with lower-case bold letters, with a_n being the nth element of $\boldsymbol{a}$; finite sets are denoted with upper-case calligraphic letters, e.g. $\mathcal{A}$; transpose and expectation are denoted with $(\cdot)^T$ and $\mathbb{E}\{\cdot\}$, respectively; probability mass functions (pmfs) and probability density functions (pdfs) are denoted with $P(\cdot)$ and $p(\cdot)$, respectively, while $P(\cdot|\cdot)$ and $p(\cdot|\cdot)$ their corresponding conditional counterparts; the complementary cumulative distribution function (ccdf) is denoted with $F(\cdot)$; the symbols $\sim$ and $\overset{a}{\sim}$ mean "distributed as" and "asymptotically distributed as"; $\mathcal{N}(\mu, \sigma^2)$ denotes a Gaussian pdf with mean μ and variance σ^2; $\mathcal{GN}(\mu, \alpha, \epsilon)$ denotes a generalized normal pdf with mean μ, scale α and shape ϵ; χ_k^2 (resp. $\chi_k^{'2}(\xi)$) denotes a chi-square (resp. a non-central chi-square) pdf with k degrees of freedom (resp. and non-centrality parameter ξ).

II. PROBLEM STATEMENT

The system model is illustrated in Fig. 1 and described in what follows. We consider a binary hypothesis test where a collection of sensors $k \in \mathcal{K} \triangleq \{1, \ldots, K\}$ are deployed in a surveillance area to monitor the absence ($\mathcal{H}_0$) or presence ($\mathcal{H}_1$) of a target of interest having a partially-specified spatial signature. In the latter case (i.e. $\mathcal{H}_1$), the target moves along a fixed direction with constant velocity and continuously radiates an unknown deterministic isotropic signal θ. Such model potentially describes scenarios including the detection of movements of troop, vehicle, equipment in battlefield surveillance, movements of birds, small animals, and insects in environmental monitoring, and car thefts in community security protection [41]. The emitted signal experiences distance-dependent path-loss and additive noise, before reaching individual sensors. The problem can be summarized as follows:

$$\begin{cases} \mathcal{H}_0: & m_k^t = w_k^t, & k \in \mathcal{K}, \\ \mathcal{H}_1: & m_k^t = \theta\, g(\boldsymbol{x}^t, \boldsymbol{s}_k) + w_k^t; & t = 1, 2 \ldots, T \end{cases} \quad (1)$$

In Eq. (1), $m_k^t \in \mathbb{R}$ denotes the kth sensor measurement at instant t and $w_k^t \in \mathbb{R}$ indicates the corresponding noise Random Variable (RV). The RVs w_k^t are assumed (a) statistically independent over space (sensors) and (b) i.i.d. over time. In detail we assume each noise RV has $\mathbb{E}\{w_k^t\} = 0$ and *unimodal symmetric*

pdf[3] $p_{w_k}(\cdot)$. We underline that reliable estimation of the sensor noise pdf(s) can be achieved based on training data.

By denoting with $\boldsymbol{x}^0 \in \mathbb{R}^d$ and $\boldsymbol{v} \in \mathbb{R}^d$ the initial target location and the corresponding velocity, respectively, the target location at time t is given by the parametric expression $\boldsymbol{x}^t = \boldsymbol{x}^0 + \boldsymbol{v}t$. Accordingly, the functional model does not consider potential fluctuations in the velocity of the target, i.e. our model assumes a constant-velocity target to be detected. Still, we highlight that the present model could easily accommodate any other kind of deterministic trajectories (e.g. constant turn or two-leg trajectory models). On the contrary, the presence of a non-negligible process noise in $\boldsymbol{v}$ would require the more flexible nearly-constant velocity model [42]. In the latter case, we expect a detection performance degradation for both G-Rao and GLR tests based on a constant-velocity assumption (due to model mismatch).

In this paper, we make the reasonable assumption that both $\boldsymbol{x}^0$ and $\boldsymbol{v}$ are *unknown*. On the other hand, $\boldsymbol{s}_k \in \mathbb{R}^d$ denotes the *known* kth sensor position, as a result of a sensor self-localization procedure [43], [44]. The pair $(\boldsymbol{x}^t, \boldsymbol{s}_k)$ *uniquely* determines the value of $g(\boldsymbol{x}^t, \boldsymbol{s}_k)$, here denoting the amplitude attenuation function (AAF)[4], which models how the signal emitted from the target at t decays as it reaches kth sensor. For instance, one relevant AAF is given by the power-law decay, namely $g(\boldsymbol{x}^t, \boldsymbol{s}_k) \triangleq 1/\sqrt{1 + (\|\boldsymbol{x}^t - \boldsymbol{s}_k\|/a)^b}$, where a and b control the (approximate) spatial signature extent and the rapidity of signal decay, respectively.

When the noise is modelled as $w_k^t \sim \mathcal{N}(0, \sigma_{w,k}^2)$, the measurement m_k^t is distributed under $\mathcal{H}_0$ as $m_k^t \,|\, \mathcal{H}_0 \sim \mathcal{N}(0, \sigma_{w,k}^2)$. Correspondingly, under $\mathcal{H}_1$, it holds $m_k^t \,|\, \mathcal{H}_1 \sim \mathcal{N}(\theta\, g(\boldsymbol{x}^t, \boldsymbol{s}_k), \sigma_{w,k}^2)$.

By looking at Eq. (1) we observe that the test is *two-sided*, namely $\{\mathcal{H}_0, \mathcal{H}_1\}$ corresponds to $\{\theta = \theta_0, \theta \neq \theta_0\}$ ($\theta_0 = 0$). More important, the *unknown* time-varying target position $\boldsymbol{x}^t$ (equivalently the nuisance parameters $\{\boldsymbol{x}^0, \boldsymbol{v}\}$) can be estimated at the FC *only* when $\theta \neq \theta_0$, i.e. when the signal is present ($\mathcal{H}_1$). This corresponds to a set of nuisance parameters which are present only under the alternative hypothesis [45].

Then, to address bandwidth- and energy-limited budget in WSNs, we assume that the kth sensor employs a (multi-level) $q(k)$-bit quantizer[5], in which the observation m_k^t is compared

---

[3]Noteworthy examples of such pdfs are the Gaussian, Laplace, Cauchy and generalized Gaussian distributions with zero mean [30].

[4]We underline that our results apply to any suitably-defined AAF describing the spatial signature of the target to be detected.

[5]Herein, for simplicity, we focus on deterministic quantizers, leaving the more general case of probabilistic quantizers [10] to future studies.

with a set of quantization thresholds $\{\tau_k(i)\}_{i=0}^{2^{q(k)}}$, determining $2^{q(k)}$ non-intersecting intervals covering the whole $\mathbb{R}$. We stress that $\tau_k(0) = -\infty$ and $\tau_k(2^{q(k)}) = +\infty$ are two *dummy* thresholds used in what follows to keep the notation compact. Precisely, the corresponding quantizer outcome is mapped into a binary codeword $\boldsymbol{b}_k^t \in \{0,1\}^{q(k)}$, where $k = 1, 2, \ldots, K$. The non-overlapping quantization intervals are associated to $q(k)$-bit binary codewords $\boldsymbol{c}(i) = \begin{bmatrix} c_1(i) & \cdots & c_{q(k)}(i) \end{bmatrix}^T$, where $c_t(i) \in \{0,1\}$.

Hence, the $q(k)$-bit quantizer of kth sensor at instant t outputs a codeword defined as:

$$\boldsymbol{b}_k^t \triangleq \begin{cases} \boldsymbol{c}(1) & -\infty < m_k^t < \tau_k(1) \\ \boldsymbol{c}(2) & \tau_k(1) \le m_k^t < \tau_k(2) \\ \vdots & \vdots \\ \boldsymbol{c}(2^{q(k)}) & \tau_k(2^{q(k)}-1) \le m_k^t < +\infty \end{cases} \quad (2)$$

We observe that herein *raw measurement quantization* (as opposed to other local sensor processing, e.g. quantization of energy statistic [11]) is pursued to keep the signal polarity in case an estimate of θ is required after detection. Still, we stress that analogous design issues would arise (i.e. nuisance parameters observable only under $\mathcal{H}_1$) in case of sensor energy quantization, with corresponding non-feasibility of the common locally most-powerful tests and the need for generalized statistics, based on Davies' approach [45]. The codeword of kth sensor is then reported to the FC via an error-prone reporting link. The communication process of *each bit* is represented by an independent BSC with (known) Bit-Error Probability (BEP) $P_{e,k}$.

A *distorted* codeword $\boldsymbol{y}_k^t$ will be then received by the FC from kth sensor at time t, whose conditional probability obeys $P(\boldsymbol{y}_k^t = \boldsymbol{c}_k(i) | \boldsymbol{b}_k^t = \boldsymbol{c}_k(j)) = G_{q(k)}(P_{e,k}, d_{i,j})$, where

$$G_{q(k)}(P_{e,k}, d_{i,j}) \triangleq P_{e,k}^{d_{i,j}} (1 - P_{e,k})^{(q(k)-d_{i,j})}, \quad (3)$$

and $d_{i,j} \triangleq d(\boldsymbol{c}_k(i), \boldsymbol{c}_k(j))$ denotes the Hamming distance between codewords $\boldsymbol{c}_k(i)$ and $\boldsymbol{c}_k(j)$.

For notational compactness, we collect the noisy codewords (viz. soft-quantized measurements) received from the sensors at time t in the set $\boldsymbol{Y}^t \triangleq \{\boldsymbol{y}_1^t \cdots \boldsymbol{y}_K^t\}$ (recall that $\boldsymbol{y}_k^t \in \{0,1\}^{q(k)}$ and thus codewords from sensors may differ in length). Similarly, the accumulated noisy codewords received from the sensors up to time $\bar{t}$ are denoted as $\boldsymbol{Y}^{1:\bar{t}} \triangleq \{\boldsymbol{Y}^1, \ldots, \boldsymbol{Y}^{\bar{t}}\}$.

Accordingly the pmf of all the observations as a function of the set of unknown parameters $\boldsymbol{\xi} \triangleq \{\theta, \boldsymbol{x}^0, \boldsymbol{v}\}$, up to a generic time $\bar{t}$ (i.e. $\boldsymbol{Y}^{1:\bar{t}}$), is then given by

$$P(\boldsymbol{Y}^{1:\bar{t}}; \underbrace{\theta, \boldsymbol{x}^0, \boldsymbol{v}}_{\boldsymbol{\xi}}) = \prod_{t=1}^{\bar{t}} \prod_{k=1}^{K} P(\boldsymbol{y}_k^t; \theta, \boldsymbol{x}^0, \boldsymbol{v}). \quad (4)$$

Clearly, $P(\boldsymbol{Y}^{1:\bar{t}}; \theta_0, \boldsymbol{x}^0, \boldsymbol{v}) = P(\boldsymbol{Y}^{1:\bar{t}}; \theta_0)$ denotes the pmf under $\mathcal{H}_0$.

The corresponding pmf of the contribution from kth sensor at generic time t can be expanded as

$$P(\boldsymbol{y}_k^t; \boldsymbol{\xi}) = \sum_{i=1}^{2^{q(k)}} P(\boldsymbol{y}_k^t | \boldsymbol{b}_k^t = \boldsymbol{c}(i)) P(\boldsymbol{b}_k^t = \boldsymbol{c}(i); \boldsymbol{\xi}). \quad (5)$$

The quantizer law reported in Eq. (2) implies the following pmf expression for $P(\boldsymbol{b}_k^t = \boldsymbol{c}(i); \boldsymbol{\xi})$

$$P(\boldsymbol{b}_k^t = \boldsymbol{c}(i); \boldsymbol{\xi}) = \Pr\{\tau_k(i-1) \le m_k^t < \tau_k(i)\} =$$
$$F_{w_k}(\tau_k(i-1) - \theta\, g(\boldsymbol{x}^t, \boldsymbol{s}_k)) - F_{w_k}(\tau_k(i) - \theta\, g(\boldsymbol{x}^t, \boldsymbol{s}_k)), \quad (6)$$

where $F_{w_k}(\cdot)$ denotes the ccdf of w_k^t.

The problem of interest in this work is (*a*) to formulate a computationally-efficient test rule based on a corresponding fusion statistic (indicated with δ and Λ, respectively) to detect the uncooperative target (as quick as possible) under constraints on error probabilities and (*b*) the design of quantizers for the *whole* WSN. Indeed, upon receiving $\boldsymbol{Y}^1, \boldsymbol{Y}^2 \ldots$, the FC can make a global decision in either (*i*) a **FSS** (waiting up to time T_f, based on a fusion statistic which capitalizes the whole batch $\boldsymbol{Y}^{1:T_f}$) or in a (*ii*) **sequential** manner (at each time instant t, based on $\boldsymbol{Y}^{1:t}$, until some exit condition is met). The aim of this paper is to investigate *both setups*, as detailed in what follows.

We highlight that the fusion rules and the (multi-bit) quantizer design obtained in this paper rely on the knowledge of the *noise* (through $P(\boldsymbol{b}_k^t = \boldsymbol{c}(j); \boldsymbol{\xi})$) and *channel models* (through $G_{q(k)}(P_{e,k}, d_{i,j})$), with optimization benefits reduced in the case of mismatch.

III. FUSION RULES DESIGN

The aim of this paper is the derivation of a (computationally) simple test deciding for $\mathcal{H}_1$ (resp. $\mathcal{H}_0$) when the statistic is above (resp. below) the threshold γ, and the design of quantizers for the *whole* WSN.

Accordingly, Section III-A details the formulation of test rules based on FSS and sequential setups (with corresponding relevant performance metrics). Then, in Section III-B, we delve into fusion statistic design, whereas in Section III-C we focus on their corresponding computational costs. Conversely, the quantizer design is tackled in later Section IV.

A. Test Rule Design

1) FSS Approach: Given a test statistic, the FC can make its decision either in a FSS or sequential fashion. In the former case, the FC first collects a specific (fixed) number of samples and then makes a final decision by the following decision rule:

$$\delta_{T_f} \triangleq \begin{cases} 1 & \text{if } \Lambda^{T_f} \ge \gamma_f, \\ 0 & \text{otherwise}. \end{cases} \quad (7)$$

where T_f denotes the number of samples, Λ^{T_f} represents the generic fusion statistic evaluated at $\bar{t} = T_f$, and γ_f denotes the decision threshold. Accordingly, the performance will be evaluated in terms of the well-known system false-alarm P_F^f

and detection P_D^{f} probabilities, defined as:

$$P_F^{\mathrm{f}} \triangleq \Pr\{\delta_{T_{\mathrm{f}}} = 1|\mathcal{H}_0\} = \Pr\{\Lambda^{T_{\mathrm{f}}} \geq \gamma_{\mathrm{f}}|\mathcal{H}_0\}, \qquad (8)$$

$$P_D^{\mathrm{f}} \triangleq \Pr\{\delta_{T_{\mathrm{f}}} = 1|\mathcal{H}_1\} = \Pr\{\Lambda^{T_{\mathrm{f}}} \geq \gamma_{\mathrm{f}}|\mathcal{H}_1\}, \qquad (9)$$

where γ_{f} represents the usual system (decision) threshold, needed to ensure a desired false-alarm rate.[6]

2) Sequential Approach: Though a multi-bit quantization has the potential advantage of better detection performance, it increases the computational burden as well. It is well known that, in many cases, the sequential test procedure can reduce the required data sample size compared to its FSS counterpart while ensuring the same detection performance. Unfortunately, both the GLR and (generalized) Rao statistics are always nonnegative in two-sided hypothesis testing. As a result, tests including both lower and upper stopping thresholds (such as the generalized sequential probability ratio test in [46]) are not applicable here. Furthermore, typical sequential tests with no upper bound on stopping time may require an excessively large number of samples in certain unfavorable realizations. To overcome these two drawbacks, following the idea in [34], herein we employ a Truncated One-sided Sequential (TOS) multi-bit test to deal with the described detection problem.

In the TOS test setup, the FC sequentially updates its test statistic based on the newly received information, until either the test statistic exceeds a prescribed threshold γ_{s} or the time horizon passes a deadline T_{s}. Specifically, the stopping rule for the TOS test based on the G-Rao (GLR) test statistic can be represented as

$$\mathcal{T} \triangleq \min\left\{\inf\left\{t > 0 : \Lambda^t \geq \gamma_{\mathrm{s}}\right\}, T_{\mathrm{s}}\right\}, \qquad (10)$$

and the decision function at the stopping time is

$$\delta_{\mathcal{T}} \triangleq \begin{cases} 1 & \text{if } \Lambda^{\mathcal{T}} \geq \gamma_{\mathrm{s}}, \\ 0 & \text{otherwise.} \end{cases} \qquad (11)$$

Clearly, the decision of the TOS test rule is delayed and equal to T_{s} when the target is absent (i.e. the case $\mathcal{H}_0$). In such a case, other than the system false-alarm and detection probabilities, also the *expected detection delay* under $\mathcal{H}_1$ is of interest, and their expressions are respectively given by [34]

$$P_F^{\mathrm{s}} \triangleq \Pr\{\delta_{\mathcal{T}} = 1|\mathcal{H}_0\}$$
$$= \Pr\{\exists\, 1 \leq t \leq T_{\mathrm{s}}, \text{ s.t. } \Lambda^t \geq \gamma_s|\mathcal{H}_0\}, \qquad (12)$$

$$P_D^{\mathrm{s}} \triangleq 1 - \Pr\{\delta_{\mathcal{T}} = 0|\mathcal{H}_1\}$$
$$= 1 - \Pr\{\forall\, 1 \leq t \leq T_{\mathrm{s}}, \ \Lambda^t < \gamma_s|\mathcal{H}_1\}, \qquad (13)$$

and

$$\bar{\mathcal{T}}_1 \triangleq \mathbb{E}[\mathcal{T}|\mathcal{H}_1]$$
$$= 1 + \sum_{t=1}^{T_{\mathrm{s}}-1} \Pr\{\Lambda^1 < \gamma_s, \ldots, \Lambda^t < \gamma_s|\mathcal{H}_1\} \qquad (14)$$

[6]Alternatively, the threshold γ_{f} can be also set to minimize the fusion error-probability [9].

To this point, we provide some quantative insights into the proposed TOS test rule. First, the expected decision delay under $\mathcal{H}_1$ is smaller than the deadline T_{s}, which is a generic feature of sequential test rules. Then considering the FSS test rule as a benchmark and let $T_{\mathrm{s}} = T_{\mathrm{f}}$, the TOS scheme may require a larger threshold to achieve an equivalent false-alarm probability, thus resulting in a larger miss-detection probability. In light of this, we prefer to set T_{s} to be slightly larger than T_{f} to avoid performance loss in miss detection. However, a larger T_{s} may bring about a longer decision delay when the decision is $\mathcal{H}_0$.

Compared with its FSS counterpart, the TOS test rule accelerates the detection speed when the target is present while always deferring the decision of $\mathcal{H}_0$, since when the decision is $\mathcal{H}_0$, the sampling time reaches T_{s} that is usually larger than the sample size of the FSS scheme. The TOS test rule appears attractive for surveillance applications, such as the noncooperative moving target detection problem considered in this work, which seeks to make a quick decision under $\mathcal{H}_1$ (which usually corresponds to the existence of an illegal object), but makes little of the importance to stop rapidly under hypothesis $\mathcal{H}_0$ (i.e., normal condition). Finally, some non-asymptotic behavior of the error probabilities and the expected decision delay of the sequential G-Rao-statistic based detector will be evaluated via simulations in Section VI.

B. Test Statistic Derivation

A common approach to handle detection in the presence of unknown parameters (viz. composite hypothesis testing) resorts to the GLR [30]. For the DD problem at hand, the corresponding decision statistic is obtained by replacing the unknown parameters $\{\theta, \boldsymbol{x}^0, \boldsymbol{v}\}$ with their ML estimates $\{\hat{\theta}, \hat{\boldsymbol{x}}^0, \hat{\boldsymbol{v}}\}$ (under $\mathcal{H}_1$) in the LR, i.e.

$$\frac{p(\boldsymbol{Y}^{1:\bar{t}}; \hat{\theta}, \hat{\boldsymbol{x}}^0, \hat{\boldsymbol{v}})}{p(\boldsymbol{Y}^{1:\bar{t}}; \theta_0)}, \qquad (15)$$

where $\theta_0 = 0$, and the ML estimates $\{\hat{\theta}, \hat{\boldsymbol{x}}^0, \hat{\boldsymbol{v}}\}$ are respectively the relevant solution of the following equation, i.e.

$$\{\hat{\theta}, \hat{\boldsymbol{x}}^0, \hat{\boldsymbol{v}}\} \triangleq \arg\max_{\theta, \boldsymbol{x}^0, \boldsymbol{v}} p(\boldsymbol{Y}^{1:\bar{t}}; \theta, \boldsymbol{x}^0, \boldsymbol{v}). \qquad (16)$$

Clearly, leveraging the explicit expression of the likelihood in Eq. (4), the test statistic in Eq. (15) can be equivalently recast into its logarithmic form as

$$\Lambda_{\mathrm{G}}^{\bar{t}} \triangleq \sum_{t=1}^{\bar{t}} \sum_{k=1}^{K} \ln \frac{P(\boldsymbol{y}_k^t; \hat{\theta}, \hat{\boldsymbol{x}}^0, \hat{\boldsymbol{v}})}{P(\boldsymbol{y}_k^t; \theta_0)}. \qquad (17)$$

Note that the MLEs of unknown parameters in Eq. (17) do not ensure a closed-form solution. In other words, searching for the solution of $\{\hat{\theta}, \hat{\boldsymbol{x}}^0, \hat{\boldsymbol{v}}\}$ in Eq. (16) may require a huge amount of computations and consequently *increases the computational burden* of its implementation.

Conversely, inspired by the approach employed in [33], [34], the G-Rao test statistic is considered here. The reason for our choice is that the typical Rao test is known to be asymptotically

equivalent to the GLRT *under the condition of weak signal* [7], but with a lower computational complexity than the latter one. As to the problem in Eq. (1), if $\boldsymbol{x}^t$ (or $\{\boldsymbol{x}_0, \boldsymbol{v}\}$) was known, the original Rao test statistic could be readily computed [30]. Unfortunately, the target trajectory $\boldsymbol{x}^t$ (or $\{\boldsymbol{x}_0, \boldsymbol{v}\}$) is unknown. However, based on the G-Rao test proposed in [33], a family of Rao test statistics can be calculated for different values of $\boldsymbol{x}^t$ (or $\{\boldsymbol{x}_0, \boldsymbol{v}\}$). Then by maximizing such family of statistics (i.e. following a "GLRT-like" approach), the G-Rao test statistic can be obtained as

$$\Lambda_{\mathrm{R}}^{\bar{t}} \triangleq \max_{\boldsymbol{x}^0, \boldsymbol{v}} \left\{ \frac{\left(\left. \frac{\partial \ln\left[p(\boldsymbol{Y}^{1:\bar{t}}; \theta, \boldsymbol{x}^0, \boldsymbol{v})\right]}{\partial \theta} \right|_{\theta=\theta_0} \right)^2}{\mathrm{I}_{\bar{t}}(\theta_0, \boldsymbol{x}^0, \boldsymbol{v})} \right\}, \quad (18)$$

where $\mathrm{I}_{\bar{t}}(\theta_0, \boldsymbol{x}^0, \boldsymbol{v})$ denotes the *Fisher Information* (FI), i.e. $\mathrm{I}_{\bar{t}}(\theta, \boldsymbol{x}^0, \boldsymbol{v}) \triangleq \mathbb{E}\left\{ \left(\frac{\partial \ln[p(\boldsymbol{Y}^{1:\bar{t}}; \theta, \boldsymbol{x}^0, \boldsymbol{v})]}{\partial \theta} \right)^2 \right\}$ evaluated at θ_0. We remark that the FI obtained satisfies the regularity condition[8] $\mathbb{E}\left\{ \left(\frac{\partial \ln[p(\boldsymbol{Y}^{1:\bar{t}}; \theta, \boldsymbol{x}^0, \boldsymbol{v})]}{\partial \theta} \right) \right\} = 0$. Hereinafter, we briefly describe the key steps needed to obtain the explicit form of the G-Rao test.

First, the numerator term in Eq. (18) (before evaluation at $\theta = \theta_0$) can be expressed as shown in Eq. (19) shown at the bottom of this page (the proof is given in Appendix A), where the auxiliary definition

$$\rho(\boldsymbol{b}_k^t = \boldsymbol{c}(i); \theta, \boldsymbol{x}^0, \boldsymbol{v}) \triangleq p_{w_k}\left(\tau_k(i-1) - \theta g\left(\boldsymbol{x}^t, \boldsymbol{s}_k\right) \right) - p_{w_k}\left(\tau_k(i) - \theta g\left(\boldsymbol{x}^t, \boldsymbol{s}_k\right) \right), \quad (20)$$

has been employed.

Secondly, exploiting the result for multi-bit quantized measurements in [37], the explicit form of the FI is obtained by replacing h_k with $g(\boldsymbol{x}^t, \boldsymbol{x}_k)$, which provides $\mathrm{I}_{\bar{t}}(\theta, \boldsymbol{x}^0, \boldsymbol{v})$ in closed Eq. (21), shown at the bottom of next page, where the definition in Eq. (20) has been again exploited.

Thus, combining Eq. (19) and Eq. (21), we obtain $\Lambda_{\mathrm{R}}^{\bar{t}}$ in closed form, shown at the bottom of next page Eq. (22). Despite the seemingly difficulty in its evaluation, $\Lambda_{\mathrm{R}}^{\bar{t}}$ can be easily evaluated as all the involved terms can be pre-computed off-line. Then, comparing Eq. (22) to Eq. (17), we notice that the G-Rao test

statistic is more computationally efficient than the GLRT, since the former does not need to estimate θ and only requires a grid search on the domains of the target initial location ($\boldsymbol{x}^0$) and velocity ($\boldsymbol{v}$).

Remarks: The target model considered in this paper contains as a special case the scenario of a *static* target with *known position*. In such a case, capitalizing the target location knowledge (i.e. no nuisance parameters in the corresponding two-sided test) and its time-invariance, the AAF can be simplified of its dependence on sensor-target distance. As a consequence, replacing $g(\boldsymbol{x}^t, \boldsymbol{s}_k)$ with a generic coefficient h_k in Eq. (22) (and simplifying the maximization over ($\boldsymbol{x}^0, \boldsymbol{v}$)) leads to exactly the same result as (13) of [37], i.e. a multi-bit Rao fusion rule for detecting a real-valued unknown signal θ.

C. Computational Complexity

Despite the seemingly evaluation difficulty, Λ_{R} can be more easily evaluated than its counterpart Λ_{G}, since G-Rao only requires a grid search on the initial location and velocity (no need for estimating θ, cf. Eq. (17) and Eq. (18)).

This is confirmed by the big-$\mathcal{O}$ notation complexity expressions reported in Table I, where $\bar{t}$ denotes the generic number of samples used in the evaluation of the fusion statistic at the FC. Specifically, in a FSS test rule $\bar{t} = T_{\mathrm{f}}$ (a single test evaluation is carried out only after *all* the samples in the batch have been collected) whereas in a TOS setup it holds $\bar{t} = 1, \dots \mathcal{T}$ (i.e. the statistic is re-evaluated at each time step till the exit time). As a result, the involved *complexity* of G-Rao in FSS setup is $\mathcal{O}(N_{\boldsymbol{x}^0} N_{\boldsymbol{v}} T_{\mathrm{f}} \sum_{k=1}^{K} 2^{q(k)})$ based on a 2-D grid, where $N_{\boldsymbol{x}^0}$ (resp. $N_{\boldsymbol{v}}$) is the number of initial position (resp. velocity) bins used. Conversely, the GLR requires a 3-D grid-based implementation, which leads in the same setup to $\mathcal{O}(N_{\theta} N_{\boldsymbol{x}^0} N_{\boldsymbol{v}} T_{\mathrm{f}} \sum_{k=1}^{K} 2^{q(k)})$, with a consequent N_{θ}-fold saving for G-Rao. Indeed, a complexity $\mathcal{O}(\bar{t} \sum_{k=1}^{K} 2^{q(k)})$ is associated to a single evaluation of both fusion statistics within the maximization (i.e. fixing ($\boldsymbol{x}^0, \boldsymbol{v}$) and ($\boldsymbol{x}^0, \boldsymbol{v}, \theta$) for Rao and GLR, respectively) when $\bar{t}$ samples have been collected by each sensor, and $q(k)$-bit quantization is employed by kth sensor. Indeed, the latter assumption implies $2^{q(k)}$ different codeword values for kth sensor at the FC.

The same complexity savings hold in the TOS case, since the complexity of GLR is $\mathcal{O}(N_{\theta} N_{\boldsymbol{x}^0} N_{\boldsymbol{v}} \frac{1}{2}\mathcal{T}(\mathcal{T}+1) \sum_{k=1}^{K} 2^{q(k)})$, whereas for G-Rao it holds $\mathcal{O}(N_{\boldsymbol{x}^0} N_{\boldsymbol{v}} \frac{1}{2}\mathcal{T}(\mathcal{T}+1) \sum_{k=1}^{K} 2^{q(k)})$. Indeed, recall that $\sum_{t=1}^{\mathcal{T}} t = (1/2)\mathcal{T}(\mathcal{T}+1)$. Accordingly, the computational complexity of both rules scales *linearly* in both the number of sensors (K) and *exponentially* in the bit resolution. Conversely, the complexity scales *linearly* (resp. *quadratically*) with number of samples in the FSS (resp. TOS) setup. Finally, we remark that the complexity associated

---

[7]That is $|\theta_1 - \theta_0| = c/\sqrt{K}$ for some constant $c > 0$, where θ_1 denotes the actual parameter value under $\mathcal{H}_1$.

[8]Indeed, the regularity condition can be rewritten $\sum_{k=1}^{K} \sum_{t=1}^{\bar{t}} \mathbb{E}\left\{ \left(\frac{\partial \ln[p(\boldsymbol{y}_k^t; \theta, \boldsymbol{x}^0, \boldsymbol{v})]}{\partial \theta} \right) \right\}$ due to time and space statistical independence. After some manipulations, each of these terms can be rewritten as $g(\boldsymbol{x}^t, \boldsymbol{s}_k) \sum_{i=1}^{2^{q(k)}} \rho(\boldsymbol{b}_k^t = \boldsymbol{c}(i); \theta, \boldsymbol{x}^0, \boldsymbol{v})$. Accordingly, each term can be shown to be *zero* as a consequence of the result $\sum_{i=0}^{2^{q(i)}} \rho(\boldsymbol{b}_k^t = \boldsymbol{c}(i); \theta, \boldsymbol{x}^0, \boldsymbol{v}) = p_{w_k}(\tau_k(0)) - p_{w_k}(\tau_k(2^{q(k)})) = 0$.

$$\left(\frac{\partial \ln\left[p(\boldsymbol{Y}^{1:\bar{t}}; \theta, \boldsymbol{x}^0, \boldsymbol{v})\right]}{\partial \theta} \right)^2 = \left(\sum_{t=1}^{\bar{t}} \sum_{k=1}^{K} \frac{g\left(\boldsymbol{x}^t, \boldsymbol{s}_k\right) \sum_{i=1}^{2^{q(k)}} P(\boldsymbol{y}_k^t | \boldsymbol{b}_k^t = \boldsymbol{c}(i)) \rho(\boldsymbol{b}_k^t = \boldsymbol{c}(i); \theta, \boldsymbol{x}^0, \boldsymbol{v})}{\sum_{i=1}^{2^{q(k)}} P(\boldsymbol{y}_k^t | \boldsymbol{b}_k^t = \boldsymbol{c}(i)) P(\boldsymbol{b}_k^t = \boldsymbol{c}(i); \theta, \boldsymbol{x}^0, \boldsymbol{v})} \right)^2. \quad (19)$$

TABLE I
THE COMPUTATIONAL COMPLEXITY OF G-RAO AND GLR RULES IN FSS AND TOS SETUPS

Setup		FSS ($\bar{t} = T_{\mathrm{f}}$)		TOS ($\bar{t} = 1, \ldots, \mathcal{T}$)	
Test Rule		G-Rao	GLR	G-Rao	GLR
Complexity		$\mathcal{O}\left(N_{\boldsymbol{x}^0} N_{\boldsymbol{v}} T_{\mathrm{f}} \sum_{k=1}^{K} 2^{q(k)}\right)$	$\mathcal{O}\left(N_{\theta} N_{\boldsymbol{x}^0} N_{\boldsymbol{v}} T_{\mathrm{f}} \sum_{k=1}^{K} 2^{q(k)}\right)$	$\mathcal{O}\left(N_{\boldsymbol{x}^0} N_{\boldsymbol{v}} \frac{1}{2}\mathcal{T}(\mathcal{T}+1) \sum_{k=1}^{K} 2^{q(k)}\right)$	$\mathcal{O}\left(N_{\theta} N_{\boldsymbol{x}^0} N_{\boldsymbol{v}} \frac{1}{2}\mathcal{T}(\mathcal{T}+1) \sum_{k=1}^{K} 2^{q(k)}\right)$

to the quantizer design in the following section is not included in the aforementioned analysis. Indeed, as shown in later Section IV, the proposed quantizer design can be carried out offline and thus does not contribute to the aforementioned (per-sample) cost.

IV. QUANTIZER DESIGN

It is worth noticing that (asymptotically-)optimal deterministic quantizers cannot be obtained for the proposed G-Rao test statistic, because no performance expressions are known in the literature for tests based on the Davies approach [45]. To this end, as done in [33], we adopt a modified version of the rationale in [17] and [20]. Specifically, it is known that the TC (i.e. knowing $\boldsymbol{x}^t$ for $t = 1, \ldots, \bar{t}$) Rao statistic $\widetilde{\Lambda}_{\mathrm{R}}^{\bar{t}}$ (*together with the corresponding* TC GLR statistic), is asymptotically (and assuming a weak signal) distributed as [30]

$$\widetilde{\Lambda}_{\mathrm{R}}^{\bar{t}} \overset{a}{\sim} \begin{cases} \chi_1^2 & \text{under } \mathcal{H}_0 \\ \chi_1'^2(\lambda_Q\left(\boldsymbol{x}^{1:\bar{t}}\right)) & \text{under } \mathcal{H}_1 \end{cases} \quad (23)$$

where the non-centrality parameter is defined as $\lambda_Q(\boldsymbol{x}^{1:\bar{t}}) \triangleq (\theta_1 - \theta_0)^2 \, \mathrm{I}_{\bar{t}}(\theta_0, \boldsymbol{x}^0, \boldsymbol{v})$ (underlining dependence on $\boldsymbol{x}^{1:\bar{t}}$ via the pair $(\boldsymbol{x}^0, \boldsymbol{v})$). Herein θ_1 denotes the true value under $\mathcal{H}_1$, whereas $\theta_0 = 0$. In detail, the above parameter is explicitly given as

$$\lambda_Q\left(\boldsymbol{x}^{1:\bar{t}}\right) = \theta_1^2 \sum_{t=1}^{\bar{t}} \sum_{k=1}^{K} \Bigg\{ g^2\left(\boldsymbol{x}^t, \boldsymbol{s}_k\right) \times$$

$$\sum_{i=1}^{2^{q(k)}} \frac{\left\{ \sum_{j=1}^{2^{q(k)}} G_{q(k)}\left(P_{e,k}, d_{i,j}\right) \rho\left(\boldsymbol{b}_k^t = \boldsymbol{c}(j); \theta_0\right) \right\}^2}{\sum_{j=1}^{2^{q(k)}} G_{q(k)}\left(P_{e,k}, d_{i,j}\right) P\left(\boldsymbol{b}_k^t = \boldsymbol{c}(j); \theta_0\right)} \Bigg\}, \quad (24)$$

where we have omitted both $\boldsymbol{x}^0$ and $\boldsymbol{v}$ in the terms $\rho(\boldsymbol{b}_k^t = \boldsymbol{c}(j); \theta_0)$ and $P(\boldsymbol{b}_k^t = \boldsymbol{c}(j); \theta_0)$, since $\theta_0 = 0$ implies $\theta_0 \, g(\boldsymbol{x}^t, \boldsymbol{v}) = 0$ (cf. Eq. (6) and Eq. (20)).

Clearly, the larger $\lambda_Q(\boldsymbol{x}^{1:\bar{t}})$, the better the $\boldsymbol{x}^{1:\bar{t}}$-clairvoyant GLR and Rao tests will perform when the target to be detected depicts a trajectory $\boldsymbol{x}^{1:\bar{t}}$. Since this property holds for each accumulated time $\bar{t}$, this observation applies to both FSS and sequential variants. Also, from inspection of Eq. (24), we observe that the non-centrality parameter $\lambda_Q(\boldsymbol{x}^{1:\bar{t}})$ is a function of the set of thresholds vectors $\boldsymbol{\tau}_k^t$, $k \in \{1, \ldots, K\}$, $t \in \{1, \ldots, \bar{t}\}$. We highlight that the generic vector is defined as $\boldsymbol{\tau}_k^t \triangleq \{\tau_k^t(i)\}_{i=1}^{2^{q(k)}-1}$, where the two boundary thresholds are obviously fixed as $\tau_k^t(0) = -\infty$ and $\tau_k^t(2^{q(k)}) = +\infty$.

As a consequence, the asymptotic detection performance of the G-Rao test (as well as the GLRT) can be optimized by solving the following optimization problem

$$\max_{\left\{\{\boldsymbol{\tau}_k^t\}_{k=1}^K\right\}_{t=1}^{\bar{t}}} \lambda_Q\left(\boldsymbol{x}^{1:\bar{t}}, \left\{\{\boldsymbol{\tau}_k^t\}_{k=1}^K\right\}_{t=1}^{\bar{t}}\right). \quad (25)$$

For this reason, with a slight abuse of notation, we will use $\lambda_Q(\boldsymbol{x}^{1:\bar{t}}, \{\{\boldsymbol{\tau}_k^t\}_{k=1}^K\}_{t=1}^{\bar{t}})$ and choose the thresholds $\{\{\boldsymbol{\tau}_k^t\}_{k=1}^K\}_{t=1}^{T}$ to maximize the aforementioned objective. In other words, by optimally choosing the quantizer thresholds $\boldsymbol{\tau}_k^t$ for the set of sensors, we can optimize the detection performance of *both* TC Rao and TC GLR tests. Indeed, their asymptotic performance coincides and solely depends on the non-centrality parameter (i.e. $\lambda_Q(\boldsymbol{x}^{1:\bar{t}})$) reported in Eq. (24). Accordingly, the optimized thresholds $\{\{(\boldsymbol{\tau}_k^t)^{\star}\}_{k=1}^K\}_{t=1}^T$ based on the considered rationale will be the *same* for both G-Rao and GLR tests.

In general, such choice would lead to optimized thresholds that will be dependent on $\boldsymbol{x}^{1:\bar{t}}$ (and thus not practical), and also imply a design coupled over space (viz. sensors) and time. However, the objective in Eq. (24) can be rewritten in the

$$\mathrm{I}_{\bar{t}}(\theta, \boldsymbol{x}^0, \boldsymbol{v}) = \sum_{t=1}^{\bar{t}} \sum_{k=1}^{K} g^2\left(\boldsymbol{x}^t, \boldsymbol{s}_k\right) \sum_{i=1}^{2^{q(k)}} \frac{\left\{ \sum_{j=1}^{2^{q(k)}} G_{q(k)}\left(P_{e,k}, d_{i,j}\right) \rho\left(\boldsymbol{b}_k^t = \boldsymbol{c}(j); \theta, \boldsymbol{x}^0, \boldsymbol{v}\right) \right\}^2}{\sum_{j=1}^{2^{q(k)}} G_{q(k)}\left(P_{e,k}, d_{i,j}\right) P\left(\boldsymbol{b}_k^t = \boldsymbol{c}(j); \theta, \boldsymbol{x}^0, \boldsymbol{v}\right)}. \quad (21)$$

$$\Lambda_{\mathrm{R}}^{\bar{t}} = \max_{(\boldsymbol{x}^0, \boldsymbol{v})} \frac{1}{\mathrm{I}_{\bar{t}}\left(\theta_0, \boldsymbol{x}^0, \boldsymbol{v}\right)} \left(\sum_{t=1}^{\bar{t}} \sum_{k=1}^{K} \frac{g\left(\boldsymbol{x}^t, \boldsymbol{s}_k\right) \sum_{i=1}^{2^{q(k)}} P(\boldsymbol{y}_k^t | \boldsymbol{b}_k^t = \boldsymbol{c}(i)) \rho(\boldsymbol{b}_k^t = \boldsymbol{c}(i); \theta_0)}{\sum_{i=1}^{2^{q(k)}} P(\boldsymbol{y}_k^t | \boldsymbol{b}_k^t = \boldsymbol{c}(i)) P(\boldsymbol{b}_k^t = \boldsymbol{c}(i); \theta_0)} \right)^2. \quad (22)$$

following form

$$\lambda_Q\left(\boldsymbol{x}^{1:\bar{t}},\left\{\{\boldsymbol{\tau}_k^t\}_{k=1}^K\right\}^{\bar{t}}_{t=1}\right)=\theta_1^2\sum_{t=1}^{\bar{t}}\sum_{k=1}^K g^2\left(\boldsymbol{x}^t,\boldsymbol{s}_k\right)A_k(\boldsymbol{\tau}_k^t)\tag{26}$$

where the explicit expression of $A_k(\boldsymbol{\tau}_k^t)$ is given as follows:

$$A_k(\boldsymbol{\tau}_k^t)\triangleq\sum_{i=1}^{2^{q(k)}}\frac{\left\{\sum_{j=1}^{2^{q(k)}}G_{q(k)}\left(P_{e,k},d_{i,j}\right)\rho\left(\boldsymbol{b}_k^t=\boldsymbol{v}(j);\theta_0\right)\right\}^2}{\sum_{j=1}^{2^{q(k)}}G_{q(k)}\left(P_{e,k},d_{i,j}\right)P\left(\boldsymbol{b}_k^t=\boldsymbol{v}(j);\theta_0\right)}.\tag{27}$$

Accordingly, by observing that both θ_1^2 and $g^2(\boldsymbol{x}^t,\boldsymbol{x}_k)$ are positive terms and are independent on the thresholds, the considered optimization can be decoupled into the following set of $\bar{t}\times K$ independent threshold design problems, which are *independent* of $\boldsymbol{x}^{1:\bar{t}}$

$$\left(\boldsymbol{\tau}_k^t\right)^\star\triangleq\arg\max_{\boldsymbol{\tau}_k^t}A_k(\boldsymbol{\tau}_k^t),\quad k=1,\dots,K;\quad t=1,\dots,\bar{t};\tag{28}$$

We remark that each problem is subject to the ordered constraints $\tau_k^t(i)<\tau_k^t(i+1)$, for $i=1,\dots2^{q(k)}-1$. Remarkably, given the independence of the objective $A_k(\cdot)$ w.r.t. the time index t, the optimized quantizer design for kth sensor arises from a static solution and does not need to be changed online (i.e. $(\boldsymbol{\tau}_k^t)^\star=\boldsymbol{\tau}_k^\star$). Accordingly, only K (decoupled) quantization problems need to be solved.

Finally, since the optimization problem described via Eq. (28) has the same form as [37, Eq. (17)], we can capitalize the same method used therein, i.e. the PSO, to search the optimal quantization thresholds in Eq. (28).

V. ASYMPTOTIC DETECTION GAINS VERSUS RESOLUTION

We now establish the TC asymptotic detection gain provided by multi-bit quantization in the FSS case. To this end, by relying on Eq. (23), we express the asymptotic detection probability P_D^{f} as a function of the asymptotic probability of false-alarm P_F^{f}:

$$P_D^{\mathrm{f}}(\lambda_{(q\to s)}(\boldsymbol{x}^{1:T_{\mathrm{f}}}),P_F^{\mathrm{f}})=\mathcal{Q}\left(\mathcal{Q}^{-1}(P_F^{\mathrm{f}}/2)\sqrt{\lambda_{(q\to s)}(\boldsymbol{x}^{1:T_{\mathrm{f}}})}\right)$$
$$+\mathcal{Q}\left(\mathcal{Q}^{-1}(P_F^{\mathrm{f}}/2)\right.$$
$$\left.+\sqrt{\lambda_{(q\to s)}(\boldsymbol{x}^{1:T_{\mathrm{f}}})}\right),\tag{29}$$

where the subscript "$(q\to s)$" indicates the adoption of sensors with s-bit resolution for quantizer. To be specific, $q\to1$ denotes one-bit quantizer and $q\to n$ with $n>1$ represents the multi-level one. Also, we recall that the above asymptotic P_D^{f} expression relies on the same assumptions required for the quantizer design in Section IV, i.e. knowledge of both (sensing) noise and (communication) channel statistics.

Based on these explicit quantities, we introduce the *Asymptotic Detection Gain* (ADG) defined in [37] to quantify the gain between a WSN employing s-bit resolution and one employing
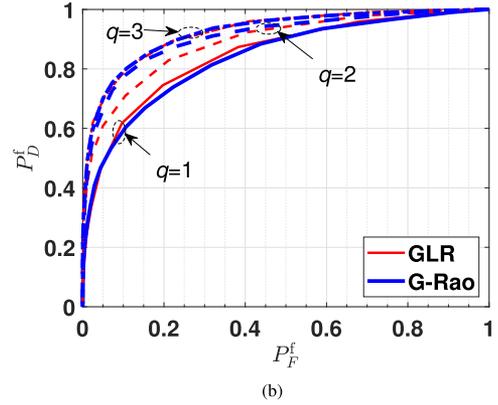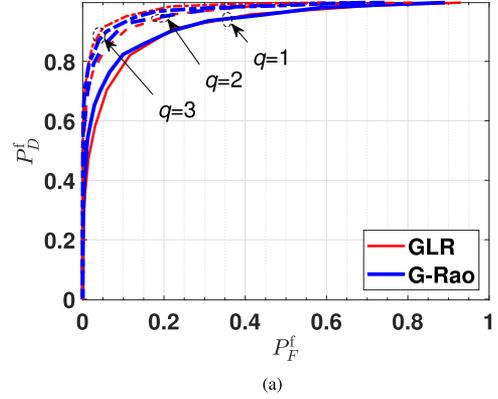

Fig. 2. P_D^{f} vs. P_F^{f} for GLRT and G-Rao with a batch size $T_{\mathrm{f}}=20$; WSN with $K=9$ sensors, $w_k\sim\mathcal{N}(0,1)$, SNR $=-3$ dB, and (a): $P_e=0$; (b): $P_e=0.1$.

t-bit resolution ($t>s$) as

$$G_d(P_F^{\mathrm{f}},\boldsymbol{x}^{1:T_{\mathrm{f}}})\triangleq$$
$$P_D^{\mathrm{f}}(\lambda_{(q\to t)}(\boldsymbol{x}^{1:T_{\mathrm{f}}}),P_F^{\mathrm{f}})-P_D^{\mathrm{f}}(\lambda_{(q\to s)}(\boldsymbol{x}^{1:T_{\mathrm{f}}}),P_F^{\mathrm{f}}),\tag{30}$$

to measure the increase in detection rate arising from the use of finer quantizers. Additionally, we also introduce the *Asymptotic Normalized Detection Gain* (ANDG) [37] as

$$\bar{G}_d(P_F^{\mathrm{f}},\boldsymbol{x}^{1:T_{\mathrm{f}}})\triangleq$$
$$\frac{P_D^{\mathrm{f}}(\lambda_{(q\to t)}(\boldsymbol{x}^{1:T_{\mathrm{f}}}),P_F^{\mathrm{f}})-P_D^{\mathrm{f}}(\lambda_{(q\to s)}(\boldsymbol{x}^{1:T_{\mathrm{f}}}),P_F^{\mathrm{f}})}{P_D^{\mathrm{f}}(\lambda_{(q\to t)}(\boldsymbol{x}^{1:T_{\mathrm{f}}}),P_F^{\mathrm{f}})},\tag{31}$$

to assess the corresponding relative increment. Obviously, both these measures can be employed to quantify the (normalized) detection gain when increasing the bit resolution from $s>0$ to t bits. Qualitative profiles of ADG and ANDG in the above relevant cases will be analyzed and commented later in Section VI for a given trajectory.

VI. NUMERICAL RESULTS

In this stage, we will resort to simulations to assess the performance of the proposed multi-bit G-Rao test, and also show some non-asymptotic properties of the multi-bit TOS approach. Specifically, we consider a 2-D space ($\boldsymbol{x}_T\in\mathbb{R}^2$) where a WSN of size $K=9$ is deployed to reveal the presence
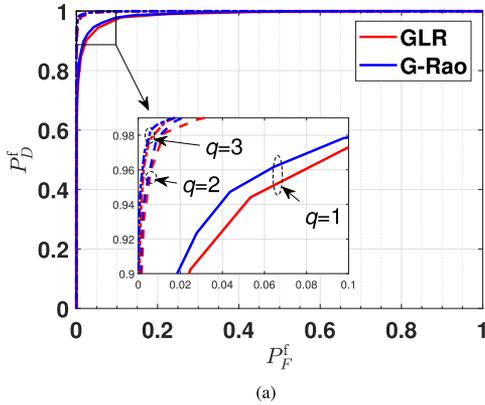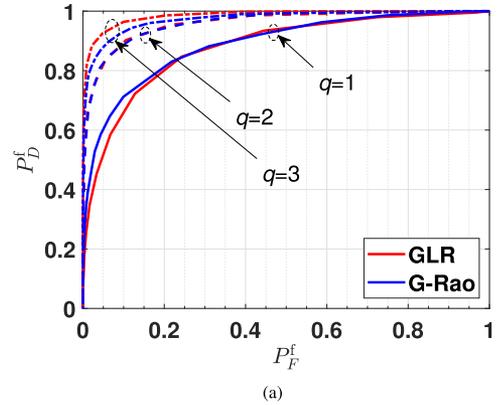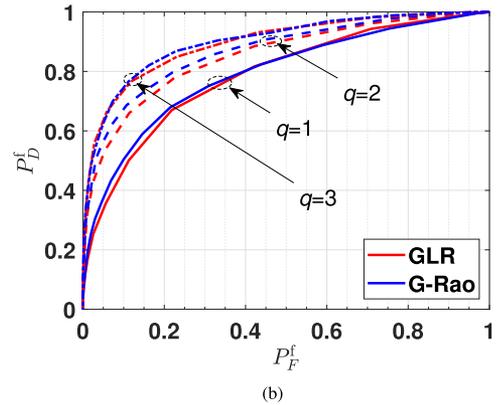
(a)
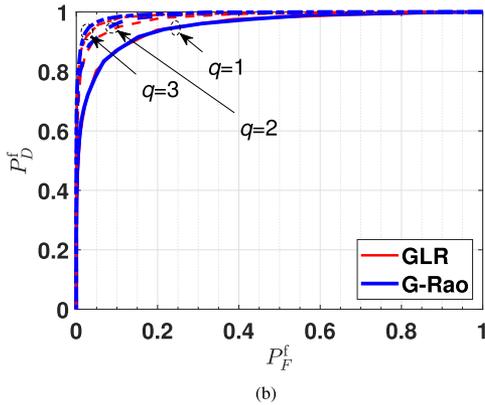
(b)

Fig. 3. P_D^f vs. P_F^f for GLRT and G-Rao with a batch size $T_f = 20$; WSN with $K = 9$ sensors, $w_k \sim \mathcal{N}(0, 1)$, SNR = 0 dB, and (a): $P_e = 0$; (b): $P_e = 0.1$.
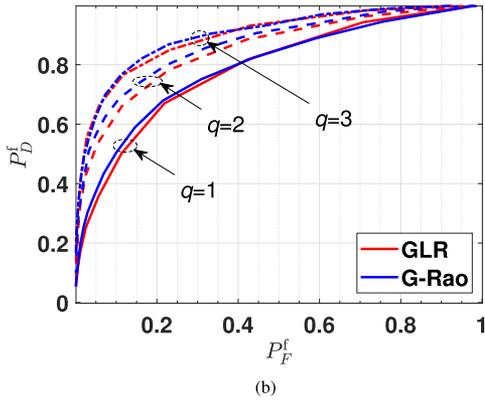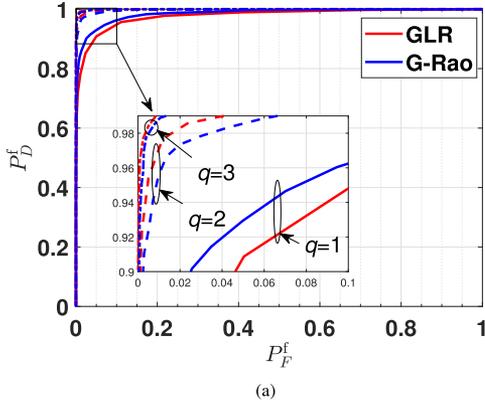

(a)

(b)

Fig. 4. P_D^f vs. P_F^f for GLRT and G-Rao with a batch size $T_f = 20$; WSN with $K = 9$ sensors, $w_k \sim \mathcal{GN}(0, \alpha, 3)$, SNR = -3 dB, and (a): $P_e = 0$; (b): $P_e = 0.1$.

of an unknown moving target with its initial position located in the (square) surveillance area $\mathcal{L} \triangleq [0, 1]^2$ and moving with velocity within $\mathcal{V} \triangleq [-0.1, 0.1]^2$. Without loss of generality, sensors are displaced in a regular grid covering $\mathcal{L}$. Concerning the sensing model, we consider a power-law AAF: $g(\boldsymbol{x}^t, \boldsymbol{s}_k) \triangleq 1/\sqrt{1 + (\|\boldsymbol{x}^t - \boldsymbol{s}_k\|/0.2)^4}$. The latter AAF model well-suits to a number of relevant WSN-based DD cases, such as electromagnetic or acoustic signatures [47].

To deeply investigate the detectors' performance under different noise pdfs, we investigate *two* relevant scenarios. Specifically, we consider the cases of (i) Gaussian noise, that is $p_w(\omega) = \frac{1}{(2\pi\sigma_w^2)^{\frac{1}{2}}} \exp(-\frac{\omega^2}{2\sigma_w^2})$ and (ii) Generalized Gaussian noise, that is $p_w(\omega) = \frac{\epsilon}{2\alpha\Gamma(1/\epsilon)} \exp[-(\frac{|\omega|}{\alpha})^\epsilon]$, respectively. We observe that scenario (i) corresponds to a widely-employed noise pdf arising due to many independent contributions (as a result of the central limit theorem), while scenario (ii) represents a flexible class of pdfs allowing to model long-tail behaviour, e.g. possibly due to outliers. It is known from [17] that one-bit quantization $(q = 1)$ $\tau^* = 0$ holds in cases of Gaussian and Generalized Gaussian (only when $0 < \epsilon \le 2$) distributions. On the other hand, when $\epsilon > 2$, $g(\tau)$ becomes bimodal and $\tau^* \neq 0$. For the mentioned reasons, to stress PSO capabilities and diversify our analysis, we will consider $\epsilon = 3$ in the GGD case. For simplicity, in what follows we assume $p_{w_k}(\cdot) = p_w(\cdot)$ and $P_{e,k} = P_e$ for all sensors, and we set $\mathbb{E}\{w_k^2\} = 1$ for both noise

pdf cases. The target signal-to-noise ratio (SNR) is defined as SNR $\triangleq \theta^2 / \mathbb{E}\{w_k^2\}$. Unless otherwise stated, we set the *true* target values as $\theta = 0.7079$ (thus SNR = -3 dB), $\boldsymbol{x}_0 = [0, 0.5]^T$, $\boldsymbol{v} = [0.02, 0.013]^T$ in the simulations to gain insight into detectors' performance. Finally, all experiments were carried out on a Windows laptop with a 2.4 GHz i9-10885H CPU and 32 GB RAM.

A. G-Rao Test Versus GLRT: Benefits of Multi-Bit Quantization

Considering the FSS test rule with a sample size $T_f = 20$, we compare multi-bit G-Rao test and GLRT performance in terms of system false alarm (P_F^f) and detection probabilities (P_D^f). Following Section III, Λ_R and Λ_G are evaluated by means of grids for $\boldsymbol{x}_0$, $\boldsymbol{v}$ and θ. Precisely, $\boldsymbol{x}_0$ and $\boldsymbol{v}$ are searched with $N_{\boldsymbol{x}^0} = N_{\boldsymbol{v}} = 100$ grid points uniformly sampling $\mathcal{L}$ and $\mathcal{V}$, respectively. Differently, the search space of θ (the target signal) is assumed to be $S_\theta \triangleq [-\bar{\theta}, \bar{\theta}]$ $(\bar{\theta} > 0)$. The grid points[9] are then chosen as $[-\boldsymbol{g}_\theta^T \ 0 \ \boldsymbol{g}_\theta^T]^T$, where $\boldsymbol{g}_\theta$ collects target strengths corresponding to SNR = $-10 : 1 : 10$ dB.

---

[9]This grid implies $N_\theta = 43$, hence a $43\times$ complexity saving is achieved by G-Rao w.r.t. GLR.

Fig. 5. P_D^{f} vs. P_F^{f} for GLRT and G-Rao with a batch size $T_{\text{f}} = 20$; WSN with $K = 9$ sensors, $w_k \sim \mathcal{GN}(0, \alpha, 3)$, $\text{SNR} = 0\,\text{dB}$, and (a): $P_e = 0$; (b): $P_e = 0.1$.

Fig. 6. (a): ADG (viz. G_d vs. P_F^{f}) and (b): ANDG (viz. $\bar{G}_d$ vs. P_F^{f}) for a WSN with $w_k \sim \mathcal{N}(0, \sigma_w^2)$, $P_e \in \{0, 0.1\}$ and different configurations (s, t).

Then, in Figs. 2 and 3 we illustrate P_D^{f} vs. P_F^{f} (viz. Receiver Operating Characteristic, ROC) in a WSN under Gaussian noise (i.e. $w_k \sim \mathcal{N}(0, \sigma_w^2)$), with $\text{SNR} = -3\,\text{dB}$ and $0\,\text{dB}$ (i.e. $\theta = 1$), respectively,. Then in Figs. 4 and 5 we illustrate analogous results pertaining to a WSN under GGD noise (i.e. $w_k \sim \mathcal{GN}(0, \alpha, 3)$) with $\text{SNR} = -3\,\text{dB}$ and $0\,\text{dB}$, respectively. In all figures, we report the results for the two BEP levels $P_e \in \{0, 0.1\}$. All the results are based on 10^5 Monte Carlo (MC) runs. Also, for each case, we report the performance with $q(k) = q \in \{1, 2, 3\}$ quantization bits, where thresholds are selected following the rationale elaborated in Section IV. We remark that $q = 1$ leads to the (FSS) one-bit G-Rao test proposed in [33] (originally referring to a stationary target though). Specifically, we use PSO with parameters $M = 100$, $\tau_{max} = 5$ and $\nu_{tol} = 10^{-6}$, corresponding to the number of particles employed, the maximum position limitation and the stop tolerance velocity, respectively [37].

It is apparent that the ROC performance of the GLR and G-Rao tests are practically the same for Gaussian noise scenario, with either $\text{SNR} = -3\,\text{dB}$ or $0\,\text{dB}$. On the other hand, in GGD case, the performance of GLRT and G-Rao test slightly differs. This is reasonable since, in general, the performance of GLRT and G-Rao test may differ in the finite sensor case. Nonetheless, the G-Rao test has the advantage of a lower computational burden with respect to the GLRT. Secondly, both fusion rules
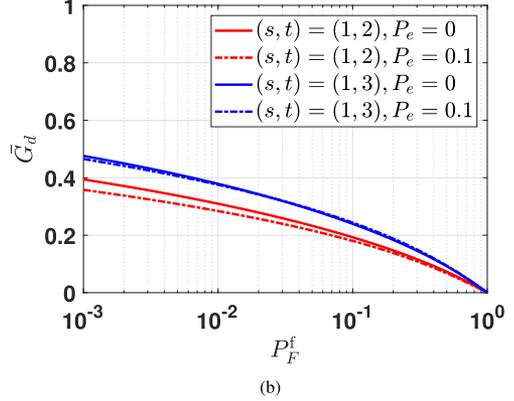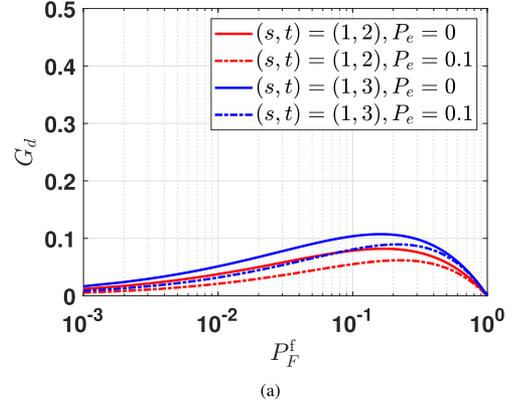
enjoy a higher detection probability (than the one-bit case) when using multi-bit quantizers. Still, the presence of channel errors (in our example $P_e = 0.1$) leads to a significant performance loss of both detectors, highlighting the need for either a higher number of sensors (K) or a longer observation interval (T_{f}).

We remark here that, other than the considered SNR values, we have also obtained the results with $\text{SNR} = -6\,\text{dB}$ (i.e. $\theta = 0.5$), $3\,\text{dB}$ (i.e. $\theta = 1.4125$) and $6\,\text{dB}$ (i.e. $\theta = 2$). Specifically, the behavior of ROC curves for $\text{SNR} = -6\,\text{dB}$ matches with the conclusions reported above. This is expected, as this case also falls within a low-SNR assumption. Conversely, in both cases $\text{SNR} = 3\,\text{dB}$ and $6\,\text{dB}$, the P_D^{f} of all curves is close to unity even when P_F^{f} is set to a very low value (close to zero), showing that both GLR and G-Rao tests perform well when the SNR is high. Because such results are consistent with the conclusions in [30], they are omitted for brevity.

B. Asymptotic Detection Gains in FSS Setup

Secondly, we investigate the asymptotic trends of WSN detection capabilities (in a FSS setup) from increasing the bit resolution by means of the ADG and the ANDG defined in Section V (Eq. (30) and Eq. (31), respectively).

To this end, in Figs. 6(a) and 6(b) we draw the aforementioned ADG (viz. $G_d(P_F^{\text{f}})$) and ANDG (viz. $\bar{G}_d(P_F^{\text{f}})$), respectively, in a WSN with $K = 9$ and Gaussian noise, e.g. $w_k \sim \mathcal{N}(0, \sigma_w^2)$.
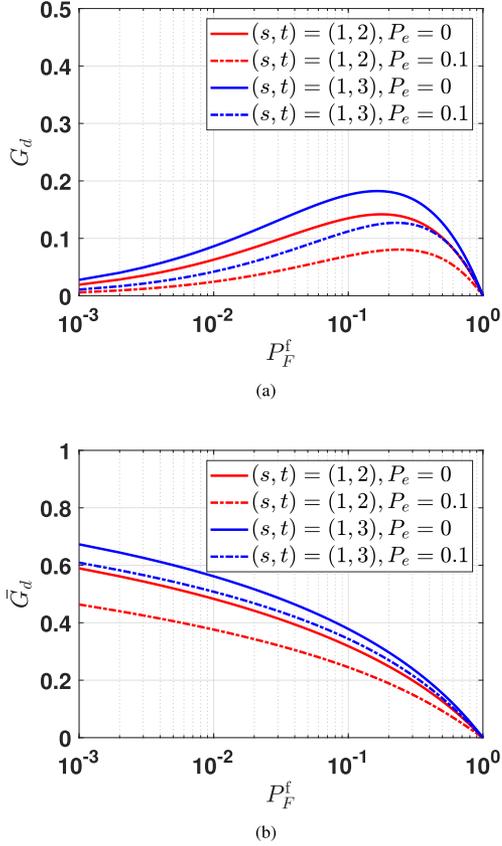
Fig. 7. (a): ADG (viz. G_d vs. P_F^{f}) and (b): ANDG (viz. $\bar{G}_d$ vs. P_F^{f}) for a WSN with $w_k \sim \mathcal{GN}(0, \alpha, 3)$, $P_e \in \{0, 0.1\}$ and different configurations (s, t).

Similarly, in Figs. 7(a) and 7(b) we illustrate the same metrics in a WSN with Generalized Gaussian noise, e.g. $w_k \sim \mathcal{GN}(0, \alpha, 3)$. The two noise scenarios are considered in conjunction with the channel cases $P_e \in \{0, 0.1\}$.

First, it is apparent a different behavior for $G_d(P_F^{\mathrm{f}})$ (unimodal) and $\bar{G}_d(P_F^{\mathrm{f}})$ (decreasing), respectively. This is explained as any gain from resolution increase has its effect decreased (resp. increased) on $G_d(P_F^{\mathrm{f}})$ as P_F^{f} tends to one (resp. to zero), since accordingly, also P_D^{f} will tend to unity (resp. to zero), independently on the WSN considered. On the other hand, in $\bar{G}_d(P_F^{\mathrm{f}})$, the trend for P_F^{f} in proximity of zero is suppressed by the normalization in Eq. (31). Secondly, compared to one-bit quantization, the implementation of multi-bit quantization can further improve detection performance. Finally, we observe that a degraded channel reasonably affects in a negative fashion because of the less informative bits received from sensors.

C. TOS Detection vs. its FSS Counterpart

Finally, we evaluate the non-asymptotic behavior of the system probabilities (P_F^{s} and P_D^{s}) and the expected detection delay ($\bar{\mathcal{T}}_1$) of the proposed multi-bit G-Rao statistic in its TOS variant (cf. Section III-A).

The following simulations are set up to guarantee that the performance of the TOS-based test rule is at least as good as the benchmarked FSS test rule in terms of system probabilities, thus
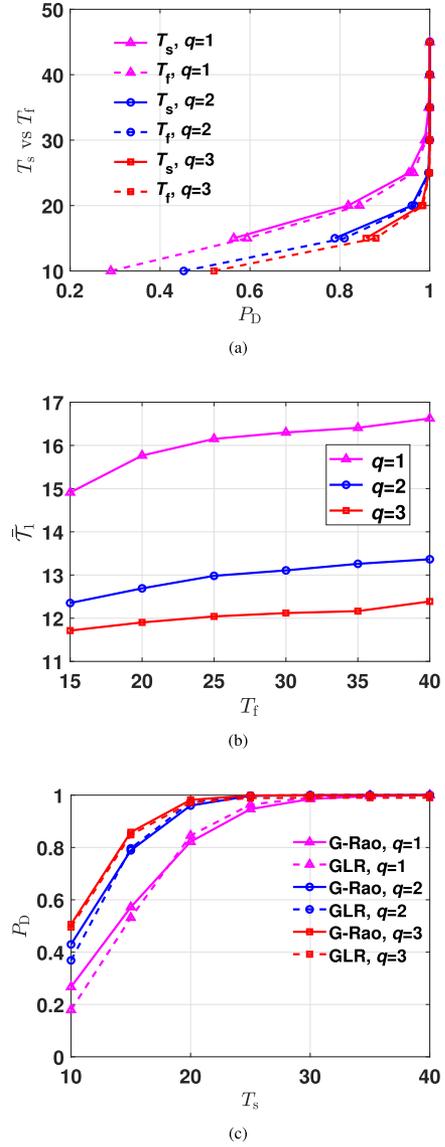

Fig. 8. (a): The required deadline of TOS compared with the sample size of FSS, when achieving similar detection probabilities, (b): The expected decision delay under $\mathcal{H}_1$ in TOS versus the sample size of FSS and (c): The detection probability versus the deadline for TOS rules either based on G-Rao or GLR test statistics.

assuring a relative fair comparison. Accordingly, for a FSS test rule with given sample size T_{f} and false-alarm probability P_F^{f}, we first obtain the system detection probability P_D^{f} by MC simulation. Next, we perform a sequence of MC simulations when the TOS test rule is employed, where we initialize $T_{\mathrm{s}} = T_{\mathrm{f}}$ and then we gradually increase T_{s} until $P_D^{\mathrm{s}} \geq P_D^{\mathrm{f}}$, with the threshold adjusted to guarantee the same false-alarm probability as the FSS test rule (i.e $P_F^{\mathrm{s}} = P_F^{\mathrm{f}}$). Both FSS and TOS variants are compared in the cases of $q(k) = q \in \{1, 2, 3\}$ quantization bits, arising from quantizers designed as proposed in Section IV. We remark that $q = 1$ leads to one-bit G-Rao tests in [33] and [34], referring to FSS and sequential setups, respectively. For brevity, in this analysis we focus on the noise case $w_k \sim \mathcal{N}(0, \sigma_w^2)$. To ensure a practical false-alarm rate, we let $P_F^{\mathrm{f}} = 10^{-3}$.
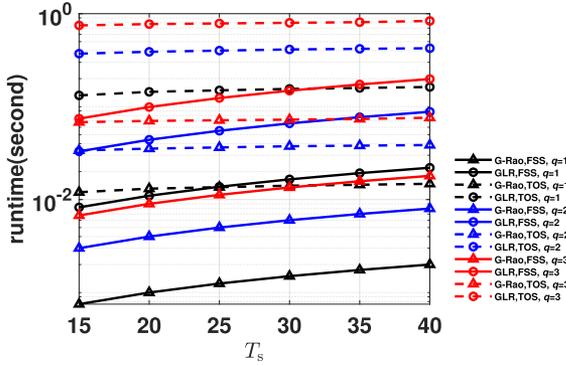
Fig. 9. The comparison of (average) CPU runtime between different test statistics.

First, in Fig. 8(a) we compare the sample size of the FSS counterpart and the minimum deadline of TOS test rule required to achieve the detection probabilities no worse than the FSS test rule. We observe that the deadline of the TOS test rule is slightly larger than the sample size of the FSS test rule. This is because the TOS test rule requires a larger threshold to achieve the same false-alarm probability as the FSS test rule; thus, more samples are needed to attain the equivalent detection probability. Conversely, Fig. 8(b) depicts the relationship between the expected detection delay under $\mathcal{H}_1$ when the TOS test rule is employed and the corresponding sample size of the FSS test rule achieving the same detection probability. It is found that the expected decision delay of TOS grows slowly with T_{f}, *significantly accelerating the detection process* when the target is present. Figs. 8(a)–(b) also show a lower sample size is required by both test rules with the increase of q, highlighting the advantage of multi-bit quantization. Then, Fig. 8(c) compares the TOS test rule based on the G-Rao statistic with that based on the GLR in terms of the detection probability P_D^s. The result illustrates the detection performance of G-Rao-based TOS test rule is very close to that of its GLR counterpart (also for different values of q considered), verifying that the G-Rao test statistic is an attractive alternative to the GLR because of less computational complexity required by the former one.

Finally, while Fig. 8(a)–(c) is executed, we record the CPU runtime spent for each test. Accordingly, Fig. 9 provides the average CPU time of running the G-Rao and GLR tests, respectively, under either FSS or TOS rules, with different quantization bits. It can be seen that the results qualitatively coincide with the computational complexity expressions reported in Table I.

VII. CONCLUSION AND FURTHER DIRECTIONS

We devised a G-Rao test for multi-bit DD of a non-cooperative moving target in WSNs. The considered model encompasses unimodal zero-mean symmetric noise, and non-identical BSCs. Our proposal constitutes a simpler alternative to the GLRT, while providing the same performance gains achieved via multi-bit quantization (over a one-bit counterpart). WSN performance was further optimized via the design of PSO-based quantizers, maximizing the asymptotic detection rate of TC Rao statistic. We also compared the performance of the TOS test rule with FSS

setup. Numerical results highlighted the multi-bit quantization design, and also showed that the TOS test rule is able to achieve the same false-alarm and miss-detection performance as its FSS counterpart with much shorter time for declaring the presence of a target, at the cost of a slightly longer time when declaring $\mathcal{H}_0$.

Future avenues of research include the (further) reduction of the computational burden for G-Rao test, by means of more efficient strategies for searching the optimal $\boldsymbol{x}^0$ and $\boldsymbol{v}$. Also, the design of G-Rao test for alternative, more general (viz. realistic) measurement and channel models is of clear interest, namely: (*a*) unknown random signal parameters [36], (*b*) vector measurement models [48], (*c*) incompletely specified noise PDFs (e.g. unknown variance), (*d*) models enjoying sparsity [24], [49], (*e*) energy-efficient censoring sensors [50] and (*f*) time-correlated reporting channels [51]. Finally, generalizing the present work to detecting (and tracking) a target with time-varying velocity is also foreseen as an interesting future topic, e.g. including the process noise in the trajectory evolution or considering more complicated deterministic models (e.g. two-leg trajectories).

APPENDIX A
PROOF OF EQ. (19) (SCORE FUNCTION)

Based on the factorization form in Eq. (4), the log-likelihood function $p(\boldsymbol{Y}^{1:\bar{t}}; \theta, \boldsymbol{x}^0, \boldsymbol{v})$ is given by

$$\ln[p\left(\boldsymbol{Y}^{1:\bar{t}}; \theta, \boldsymbol{x}^0, \boldsymbol{v}\right)] = \sum_{t=1}^{\bar{t}} \sum_{k=1}^{K} \ln P(\boldsymbol{y}_k^t; \theta, \boldsymbol{x}^0, \boldsymbol{v}) \quad (32)$$

Accordingly, the derivative with respect to θ can be written as

$$\frac{\partial \ln\left[p\left(\boldsymbol{Y}^{1:\bar{t}}; \theta, \boldsymbol{x}^0, \boldsymbol{v}\right)\right]}{\partial \theta} = \sum_{t=1}^{\bar{t}} \sum_{k=1}^{K} \frac{P'\left(\boldsymbol{y}_k^t; \theta, \boldsymbol{x}^0, \boldsymbol{v}\right)}{P\left(\boldsymbol{y}_k^t; \theta, \boldsymbol{x}^0, \boldsymbol{v}\right)} =$$

$$\sum_{t=1}^{\bar{t}} \sum_{k=1}^{K} \frac{g(\boldsymbol{x}^t, \boldsymbol{s}_k) \sum_{i=1}^{2^{q(k)}} P(\boldsymbol{y}_k^t|\boldsymbol{b}_k^t=\boldsymbol{c}(i)) \, \rho(\boldsymbol{b}_k^t=\boldsymbol{c}(i); \theta, \boldsymbol{x}^0, \boldsymbol{v})}{\sum_{i=1}^{2^{q(k)}} P(\boldsymbol{y}_k^t|\boldsymbol{b}_k^t=\boldsymbol{c}(i)) \, P(\boldsymbol{b}_k^t=\boldsymbol{c}(i); \theta, \boldsymbol{x}^0, \boldsymbol{v})}, \quad (33)$$

where $P'(\boldsymbol{y}_k^t; \cdot)$ denotes the derivative of $P(\boldsymbol{y}_k; \cdot)$ with respect to θ and, also, we have exploited the definition:

$$\rho(\boldsymbol{b}_k^t = \boldsymbol{c}(i); \theta, \boldsymbol{x}^0, \boldsymbol{v}) \triangleq p_{w_k}\left(\tau_k(i-1) - \theta g\left(\boldsymbol{x}^t, \boldsymbol{s}_k\right)\right)$$
$$- p_{w_k}\left(\tau_k(i) - \theta g\left(\boldsymbol{x}^t, \boldsymbol{s}_k\right)\right) \quad (34)$$

As a consequence, based on Eq. (33), the desired result in Eq. (19) is obtained by simple squaring operation. This ends the proof.

REFERENCES

[1] R. R. Tenney and N. R. Sandell, "Detection with distributed sensors," *IEEE Trans. Aerosp. Elect. Syst.*, vol. AES-17, no. 4, pp. 501–510, Jul. 1981.

[2] H. Kushner and A. Pacut, "A simulation study of a decentralized detection problem," *IEEE Trans. Autom. Control*, vol. 27, no. 5, pp. 1116–1119, Oct. 1982.

[3] R. S. Blum, S. A. Kassam, and H. V. Poor, "Distributed detection with multiple sensors II. Advanced topics," *Proc. IEEE*, vol. 1997, no. 1, pp. 64–79, Jan. 1997.

[4] I. F. Akyildiz, W. Su, Y. Sankarasubramaniam, and E. Cayirci, "A survey on sensor networks," *IEEE Commun. Mag.*, vol. 40, no. 8, pp. 102–114, Aug. 2002.

[5] J.-J. Xiao and Z.-Q. Luo, "Decentralized estimation in an inhomogeneous sensing environment," *IEEE Trans. Inf. Theory*, vol. 51, no. 10, pp. 3564–3575, Oct. 2005.

[6] R. Niu and P. K. Varshney, "Joint detection and localization in sensor networks based on local decisions," in *Proc. 40th Asilomar Conf. Signals, Syst. Comput.*, 2006, pp. 525–529.

[7] B. Chen, L. Tong, and P. K. Varshney, "Channel-aware distributed detection in wireless sensor networks," *IEEE Signal Process. Mag.*, vol. 23, no. 4, pp. 16–26, Jul. 2006.

[8] T. Wu and Q. Cheng, "Distributed estimation over fading channels using one-bit quantization," *IEEE Trans. Wireless Commun.*, vol. 8, no. 12, pp. 5779–5784, Dec. 2009.

[9] D. Ciuonzo, G. Romano, and P. Salvo Rossi, "Channel-aware decision fusion in distributed MIMO wireless sensor networks: Decode-and-fuse vs. decode-then-fuse," *IEEE Trans. Wireless Commun.*, vol. 11, no. 8, pp. 2976–2985, Aug. 2012.

[10] S. Kar, H. Chen, and P. K. Varshney, "Optimal identical binary quantizer design for distributed estimation," *IEEE Trans. Signal Process.*, vol. 60, no. 7, pp. 3896–3901, Jul. 2012.

[11] D. Ciuonzo and P. Salvo Rossi, "Quantizer design for generalized locally optimum detectors in wireless sensor networks," *IEEE Wireless Commun. Lett.*, vol. 7, no. 2, pp. 162–165, Apr. 2018.

[12] D. Li, K. D. Wong, Y. H. Hu, and A. M. Sayeed, "Detection, classification, and tracking of targets," *IEEE Signal Process. Mag.*, vol. 19, no. 2, pp. 17–29, Mar. 2002.

[13] J.-F. Chamberland and V. V. Veeravalli, "Decentralized detection in sensor networks," *IEEE Trans. Signal Process.*, vol. 51, no. 2, pp. 407–416, Feb. 2003.

[14] A. R. Reibman and L. L. W. Nolte, "Optimal detection and performance of distributed sensor systems," *IEEE Trans. Aerosp. Electron. Syst.*, vol. AES-23, no. 1, pp. 24–30, Jan. 1987.

[15] I. Y. Hoballah and P. K. Varshney, "Distributed Bayesian signal detection," *IEEE Trans. Inf. Theory*, vol. 35, no. 5, pp. 995–1000, Sep. 1989.

[16] R. Viswanathan and P. K. Varshney, "Distributed detection with multiple sensors - Part I: Fundamentals," *Proc. IEEE*, vol. 85, no. 1, pp. 54–63, Jan. 1997.

[17] D. Ciuonzo, G. Papa, G. Romano, P. Salvo Rossi, and P. Willett, "One-bit decentralized detection with a Rao test for multisensor fusion," *IEEE Signal Process. Lett.*, vol. 20, no. 9, pp. 861–864, Sep. 2013.

[18] D. Ciuonzo, G. Romano, and P. Salvo Rossi, "Optimality of received energy in decision fusion over Rayleigh fading diversity MAC with non-identical sensors," *IEEE Trans. Signal Process.*, vol. 61, no. 1, pp. 22–27, Jan. 2013.

[19] J. Fang and H. Li, "Distributed estimation of Gauss-Markov random fields with one-bit quantized data," *IEEE Signal Process. Lett.*, vol. 17, no. 5, pp. 449–452, May 2010.

[20] J. Fang, Y. Liu, H. Li, and S. Li, "One-bit quantizer design for multisensor GLRT fusion," *IEEE Signal Process. Lett.*, vol. 20, no. 3, pp. 257–260, Mar. 2013.

[21] R. Niu, P. K. Varshney, and Q. Cheng, "Distributed detection in a large wireless sensor network," *Inf. Fusion*, vol. 7, no. 4, pp. 380–394, 2006.

[22] A. Shoari and A. Seyedi, "Detection of a non-cooperative transmitter in Rayleigh fading with binary observations," in *Proc. IEEE Mil. Commun. Conf. (MILCOM)*, 2012, pp. 1–5.

[23] G. Wang, J. Zhu, R. S. Blum, P. Willett, S. Marano, V. Matta, and P. Braca, "Signal amplitude estimation and detection from unlabeled binary quantized samples," *IEEE Trans. Signal Process.*, vol. 66, no. 16, pp. 4291–4303, Aug. 2018.

[24] H. Zayyani, F. Haddadi, and M. Korki, "Double detector for sparse signal detection from one-bit compressed sensing measurements," *IEEE Signal Process. Lett.*, vol. 23, no. 11, pp. 1637–1641, Nov. 2016.

[25] X. Wang, G. Li, and P. K. Varshney, "Detection of sparse stochastic signals with quantized measurements in sensor networks," *IEEE Trans. Signal Process.*, vol. 67, no. 8, pp. 2210–2220, Apr. 2019.

[26] S. Laitrakun, "Decision fusion for composite hypothesis testing in wireless sensor networks over a shared and noisy collision channel," *Int. J. Distrib. Sensor Netw.*, vol. 16, no. 7, 2020, Art. no. 1550147720940204.

[27] D. Ciuonzo, S. H. Javadi, A. Mohammadi, and P. S. Rossi, "Bandwidth-constrained decentralized detection of an unknown vector signal via multisensor fusion," *IEEE Trans. Signal Inf. Process. Netw.*, vol. 6, pp. 744–758, Nov. 2020, doi: 10.1109/TSIPN.2020.3037832.

[28] P. Willett, T. L. Ogle, W. Blair, P. Miceli, and S. Marano, "Testing unbiasedness of testing a sequence of tests," in *Proc. IEEE 8th Int. Workshop Comput. Adv. Multi-Sensor Adaptive Process. (CAMSAP)*, 2019, pp. 539–543.

[29] A. Ghobadzadeh and R. S. Adve, "Separating function estimation test for binary distributed radar detection with unknown parameters," *IEEE Trans. Aerosp. Elect. Syst.*, vol. 55, no. 3, pp. 1357–1369, Jun. 2019.

[30] S. M. Kay, *Fundamentals of Statistical Signal Processing, Volume 2: Detection Theory*. Englewood Cliffs, NJ, USA: Prentice Hall, Jan. 1998.

[31] R. C. Farias, E. Moisan, and J.-M. Brossier, "Optimal asymmetric binary quantization for estimation under symmetrically distributed noise," *IEEE Signal Process. Lett.*, vol. 21, no. 5, pp. 523–526, May 2014.

[32] G. Wang, J. Zhu, and Z. Xu, "Asymptotically optimal one-bit quantizer design for weak-signal detection in generalized Gaussian noise and lossy binary communication channel," *Signal Process.*, vol. 154, no. 1, pp. 207–216, 2018.

[33] D. Ciuonzo, P. Salvo Rossi, and P. Willett, "Generalized Rao test for decentralized detection of an uncooperative target," *IEEE Signal Process. Lett.*, vol. 24, no. 5, pp. 678–682, May 2017.

[34] L. Hu, J. Zhang, X. Wang, S. Wang, and E. Zhang, "Decentralized truncated one-sided sequential detection of a non-cooperative moving target," *IEEE Signal Process. Lett.*, vol. 25, no. 10, pp. 1490–1494, Oct. 2018.

[35] D. Ciuonzo, P. S. Rossi, and P. K. Varshney, "Distributed detection in wireless sensor networks under multiplicative fading via generalized score tests," *IEEE Internet Things J.*, vol. 8, no. 11, pp. 9059–9071, Jun. 2021.

[36] F. Gao, L. Guo, H. Li, J. Liu, and J. Fang, "Quantizer design for distributed GLRT detection of weak signal in wireless sensor networks," *IEEE Trans. Wireless Commun.*, vol. 14, no. 4, pp. 2032–2042, Apr. 2015.

[37] X. Cheng, D. Ciuonzo, and P. Salvo Rossi, "Multi-bit decentralized detection through fusing smart & dumb sensors based on Rao test," *IEEE Trans. Aerosp. Elect. Syst.*, vol. 56, no. 2, pp. 1391–1405, Apr. 2020.

[38] A. I. F. Vaz and L. N. Vicente, "A particle swarm pattern search method for bound constrained global optimization," *J. Glob. Optim.*, vol. 39, no. 2, pp. 197–219, 2007.

[39] D. Ciuonzo and P. Salvo Rossi, "Distributed detection of a non-cooperative target via generalized locally-optimum approaches," *Inf. Fusion*, vol. 36, pp. 261–274, 2017.

[40] X. Cheng, D. Ciuonzo, P. Salvo Rossi, X. Wang, and L. Shi, "Multi-bit decentralized detection of a non-cooperative moving target through a generalized Rao test," in *Proc. IEEE 11th Sensor Array Multichannel Signal Process. Workshop (SAM)*, 2020, pp. 1–5.

[41] I. F. Akyildiz, W. Su, and Y. Sankarasubramaniam, "Wireless sensor networks: A survey," *Comput. Netw.*, vol. 38, no. 4, pp. 393–422, 2002.

[42] Y. Bar-Shalom, T. Kirubarajan, and X. R. Li, *Estimation With Applications to Tracking and Navigation*. New York, NY, USA: Wiley, 2002.

[43] N. Patwari, J. N. Ash, S. Kyperountas, A. O. Hero, R. L. Moses, and N. S. Correal, "Locating the nodes: cooperative localization in wireless sensor networks," *IEEE Signal Process. Mag.*, vol. 22, no. 4, pp. 54–69, Jul. 2005.

[44] A. Conti, S. Mazuelas, S. Bartoletti, W. C. Lindsey, and M. Z. Win, "Soft information for localization-of-things," *Proc. IEEE*, vol. 107, no. 11, pp. 2240–2264, Nov. 2019.

[45] R. D. Davies, "Hypothesis testing when a nuisance parameter is present only under the alternative," *Biometrika*, vol. 74, no. 1, pp. 33–43, 1987.

[46] S. Li, X. Li, X. Wang, and J. Liu, "Decentralized sequential composite hypothesis test based on one-bit communication," *IEEE Trans. Inf. Theory*, vol. 63, no. 6, pp. 3405–3424, Jun. 2017.

[47] R. Niu and P. K. Varshney, "Performance analysis of distributed detection in a random sensor field," *IEEE Trans. Signal Process.*, vol. 56, no. 1, pp. 339–349, Jan. 2008.

[48] J. Fang, X. Li, H. Li, and L. Huang, "Precoding for decentralized detection of unknown deterministic signals," *IEEE Trans. Aerosp. Electron. Syst.*, vol. 50, no. 3, pp. 2116–2128, Jul. 2014.

[49] H. Zayyani, M. Korki, and F. Marvasti, "A distributed 1-bit compressed sensing algorithm robust to impulsive noise," *IEEE Commun. Lett.*, vol. 20, no. 6, pp. 1132–1135, Jun. 2016.

[50] C. Rago, P. Willett, and Y. Bar-Shalom, "Censoring sensors: A low-communication-rate scheme for distributed detection," *IEEE Trans. Aerosp. Electron. Syst.*, vol. 32, no. 2, pp. 554–568, Apr. 1996.

[51] N. Biswas, P. Ray, and P. K. Varshney, "Distributed detection over channels with memory," *IEEE Signal Process. Lett.*, vol. 22, no. 12, pp. 2494–2498, Dec. 2015.

Xu Cheng (Member, IEEE) received the B.Sc. degree in communication engineering, the M.Sc. and the Ph.D. degrees in information and communication engineering, in 2009, 2011, and 2016, respectively, from the National University of Defense Technology, Changsha, China.

From October 2014 to October 2015, he was a Visiting Student with the University of Naples "*Federico II*," Naples, Italy. Since June 2016, He has been working as an Assistant Professor with the Policer College of PAP, Chengdu, China. He is currently also taking a Postdoctoral position with the School of Electronics and Communication Engineering, Shenzhen Campus of Sun Yat-sen University, Shenzhen, China. His research interests include statistical signal processing, with emphasis on the application of radar systems and wireless sensor networks (WSNs).

Domenico Ciuonzo (Senior Member, IEEE) received the Ph.D. degree from the University of Campania Luigi Vanvitelli, Italy, and from 2011, he has held several visiting Researcher appointments. He is currently an Assistant Professor with the University of Napoli Federico II, Naples, Italy. His research interests include data fusion, Internet of Things, network analytics and Machine Learning. Since 2014, he has been the Editor of several IEEE, IET and ELSEVIER journals. He was the recipient of two best paper awards (IEEE ICCCS 2019 and *Elsevier Computer Networks* 2020), the 2019 Exceptional Service award from IEEE Aerospace and Electronic Systems Society, and the 2020 Early-Career Technical Achievement award from IEEE Sensors Council for sensor networks/systems.

Pierluigi Salvo Rossi (Senior Member, IEEE) was born in Naples, Italy, in 1977. He received the Dr. Eng. degree (*summa cum laude*) in telecommunications engineering and the Ph.D. degree in computer engineering from the University of Naples "*Federico II*," Naples, Italy, in 2002 and 2005, respectively. He is currently a Full Professor and the Deputy Head with the Department Electronic Systems, Norwegian University of Science and Technology (NTNU), Trondheim, Norway. He is also a part-time Research Scientist with the Department Gas Technology, SINTEF Energy Research, Norway.

Previously, he worked with the University of Naples "*Federico II*," Italy, with the Second University of Naples, Italy, with NTNU, Norway, and with Kongsberg Digital AS, Norway. He held visiting appointments with Drexel University, USA, Lund University, Sweden, NTNU, Norway, and Uppsala University, Sweden.

His research interests include the areas of communication theory, data fusion, machine learning and signal processing. Prof. Salvo Rossi was awarded as the Exemplary Senior Editor of the IEEE COMMUNICATIONS LETTERS. He is (or has been) in the Editorial Board of the IEEE COMMUNICATIONS LETTERS, the IEEE OPEN JOURNAL OF THE COMMUNICATIONS SOCIETY, the IEEE TRANSACTIONS ON SIGNAL AND INFORMATION PROCESSING OVER NETWORKS, the IEEE SENSORS JOURNAL, and the IEEE TRANSACTIONS ON WIRELESS COMMUNICATIONS.

Xiaodong Wang (Fellow, IEEE) received the Ph.D. degree in electrical engineering from Princeton University, Princeton, NJ, USA. He is a Professor of Electrical Engineering with Columbia University in New York City, NY, USA. Dr. Wang's research interests include the general areas of computing, signal processing and communications, and he has published extensively in these areas. Among his publications is a book entitled "*Wireless Communication Systems: Advanced Techniques for Signal Reception*," published by Prentice Hall in 2003. His current research interests include wireless communications, statistical signal processing, and genomic signal processing. Dr. Wang was the recipient of the 1999 NSF CAREER Award, the 2001 IEEE Communications Society and Information Theory Society Joint Paper Award, and the 2011 IEEE Communication Society Award for Outstanding Paper on New Communication Topics. He was an Associate Editor for the IEEE TRANSACTIONS ON COMMUNICATIONS, the IEEE TRANSACTIONS ON WIRELESS COMMUNICATIONS, the IEEE TRANSACTIONS ON SIGNAL PROCESSING, and the IEEE TRANSACTIONS ON INFORMATION THEORY. He is listed as an ISI Highly-cited Author.

Wei Wang received the Ph.D. degree in information and communication engineering from the National University of Defense Technology, Changsha, China, in 2003. He is currently an Professor with the School of Electronics and Communication Engineering, Sun Yat-sen University, Shenzhen, China. His research interests include signal processing and electromagnetic environment effects, electronic information system modeling simulation and evaluation.